Experimental and numerical study on the performance of the smooth-land labyrinth seal

A Szymanski[1], S Dykas[1], W Wróblewski[1], M Majkut[1] and M Strozik[1]

[1] Silesian University of Technology, Institute of Power Engineering and Turbomachinery, ul. Konarskiego 18, 44-100 Gliwice, Poland

E-mail: Artur.Szymanski@polsl.pl

Abstract. In turbomachinery the secondary flow system includes flow phenomena occurring outside the main channel, where the gaseous medium performs work on blades. Secondary air distribution constitutes a very complex and closely interrelated system that affects most of the gas turbine components. One of the most important examples of the secondary flow is leakage occurring in seals, e.g. at the rotor and stator tips, on the shaft or on the sides of the blade rim. Owing to its simplicity, low price, easy maintenance and high temperature capability, the labyrinth seal is a prime sealing solution that may be selected from numerous types of sealing structures applied in turbomachinery. For this reason, an experimental study of this particular structure has been carried out. The paper presents leakage performance of the smooth-land labyrinth seal.

1. Introduction

The continuous efforts to reduce emissions of pollutants and improve the reliability, comfort and safety of the operation of aircraft engines force designers and scientists to implement new structural solutions. One important way for enhancing energy conversion efficiency in turbine engines is to improve and perfect the sealing operating conditions. The sealing type selection affects not only the size of leakage but also the temperature distribution downstream the stage, the character of the main flow, the entire system fuel consumption, the dynamics of the system operation, as well as the risk of the creep phenomenon or of a decrease in the engine thrust. The results presented in [1] may serve as an example here. They indicate that a rise in the air flow through sealing from 3.5% to 4.5%, calculated as the main flow percentage (a relative 50% rise), involves an increase in the turbine outlet temperature by 15°C. This in turn decreases durability by approximately 30% due to the risk of creep occurrence [1].

Many different kinds of sealing are used in turbomachinery. Such seals comprise the following types: brush seals, finger seals, leaf seals, graphite seals (contact seals) as well as labyrinth, foil, gas and liquid seals (non-contact). Labyrinth seals are characterized by a very simple design and are the most common turbomachinery sealing type. However, the leakage size is big compared to other solutions. Due to that fact, turbomachinery labyrinth seals have been the focus of interest of numerous academic and research centres for many years. The works undertaken in them, both experimental and numerical [2], have concentrated mainly on determining the impact of geometrical parameters on leakage, distribution of pressure [3], temperature or propagation of aeroacoustic phenomena. In experiment, most researchers focus on stationary configurations, where the motion of the rotor with the labyrinth seal relative to the casing is ignored. In experimental works [4], [5] it is proved that such simplification may be assumed if the flow velocity over the labyrinth seal fin, c_{ax}, is higher than the

rotor tangential velocity, u – in this case stationary test rigs simulate the flow behaviour correctly and the condition $u/c_{ax} < 1$ is satisfied. However, if the above-mentioned condition $u/c_{ax} < 1$ is not met and a substantial increase occurs in the mass flow difference between the stationary model and the rotating one. In most of the cases, assumption of non- rotating test rig gives satisfactory results. Researchers comparing behaviour of labyrinth seals test rigs with and without rotation pay attention to static pressure uniformity in circumferential direction. The works mentioned above also prove that the mass flow through the seal depends on many parameters, such as the inlet pressure, the inlet temperature, the Reynolds number, the angle of inflow onto the seal (initial preswirl), the pressure ratio, the seal relative motion and the architecture of the seal itself – the size of the clearance over the labyrinth fin in particular. In experiments carried out on stationary test rigs [6] [7] [8] the observed parameters are the dimensionless mass flow rate and the temperature and pressure distribution along the seal structure. These parameters make it possible to determine the loss coefficient distribution. Both high pressure feeding system (where test rig was supplied with air at pressure higher than ambient) and vacuum feeding system were used for test stands in the presented works. In all cases the authors emphasize the importance of the measurement of the clearance size as the parameter with the biggest impact on the measuring uncertainty. Under the work mentioned herein, a concept is used of feeding the measuring stand with air with ambient temperature at a stationary – axial architecture of the sealing. The air is sucked by the air blower, working as a vacuum pump, into a vessel where the set pressure value prevails. The sealing architecture maintains all dimensions of the fins and of the clearance, as well as the shape of the element over the fins. This paper presents the approach and results of experimental testing carried out on an in-house stationary (the labyrinth does not move) measuring test rig of the Institute of Power Engineering and Turbomachinery (IPET) of the Silesian University of Technology (SUT). The aim of the tests was to establish the impact of the clearance size on leakage and the static pressure distribution along the labyrinth structure. The experimental research was supported by CFD simulations by means of Ansys CFX commercial package.

2. Experimental facility

The experimental part of the testing was performed using the air installation in the Turbomachinery Laboratory of the Institute of Power Engineering and Turbomachinery of the Silesian University of Technology. The installation includes a Roots air blower with the output of 600 Nm^3/min (0.2 kg/s), a 3 m^3 pressure vessel and a pipeline system connecting the air installation to the research stand equipped with a measuring system. The system main components and the measuring instrumentation calibration procedures are described in detail in the next subsections. The minimum achievable pressure at the air blower inlet is 50 kPa(a). The total capacity of the installation (vessel and pipelines) exceeds 3.5 m3, which is relatively big compared to the expected volume flow rates, but such dimensions are indispensable to maintain stable and repeatable pressure distributions at the measurement stand inlet. Fig. 1 presents a simplified diagram of the installation. In Table 1 each part of the installation is explained. The diameter of the pipelines is DN100, which ensures a low flow velocity and small pressure losses. Secondary air (Fig. 1) is sucked in from the surroundings through the DN100 and DN 50 with throttling valve. The valve makes it possible to additionally regulate the pressure value in the vessel. The valve is controlled by an electric actuator, which allows a precise and repeatable setting of the opening angle which is remote-adjusted from the measuring system. On the stand side, the air is sucked in through an inlet preceded by a pipe which is 4 m long, which makes it possible to create appropriate conditions for the mass flow measurement upstream the test rig. After the air passes through the stand, it gets into the vessel and then – through the blower – into the environment. Mass flow evaluation is placed at inlet pipe, 3m downstream the pipe inlet.

2.1. Test rig

A stationary test rig was designed to carry out experimental testing of the flow through labyrinth sealing using a stationary linear model of the labyrinth seal. Details of the stand are presented in Figures 1 and 2. The stand is composed of 3 main elements: the inlet channel, the outlet channel and the main chamber where the tested labyrinth sealing structures are installed. As it can be seen, the inlet channel is much longer than the outlet one. This is dictated by the channel opening angle of 7°. This

opening value ensures smooth transition from a small diameter, DN100, to a big one without the risk of the separation phenomenon arising in the boundary layer. The outlet channel is much shorter. On the side walls of the measuring chamber there is an inspection peephole with a window made of BK7 optical glass, which allows measurements by means of optical methods such as Laser Doppler Anemometry. The interior dimensions of the chamber are (L x H x W) 478x240x240mm. Mentioned width of test section is more than 200 times higher than examined clearances, which minimizes the effect of side walls on the main flow. Fig. 3 presents an analysed model of the seal, with placement of pressure taps, and main dimensions. Relative values of the most important dimensions are presented in Table 2. In presented study, pressure distribution is measured on upper wall only. In Fig. 3, place of pressure measurement is coloured red. Black arrow shows place of static pressure measurement, which is used for operating pressure ratio evaluation. Pressure ratio is defined as the ratio of inlet total pressure to static pressure measured in presented point. It is described by the following equation:

$$\pi = \frac{p_{0,in}}{p_{s,16}} \tag{1}$$

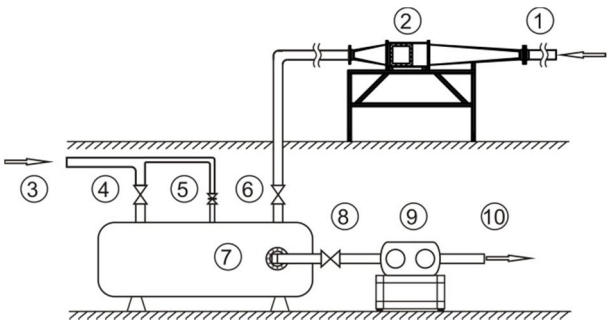

Figure 1. Experimental installation intended for the turbine seal testing in the IPET of the SUT.

Table 1. Installation description

Point	
1	Test rig inlet (mass flow measurement)
2	Test rig
3	Secondary air inlet
4	Cut-off valve
5	Remote controlled valve
6	Cut-off valve
7	3 m^3 vessel
8	Cut-off valve
9	Roots air blower
10	Outlet

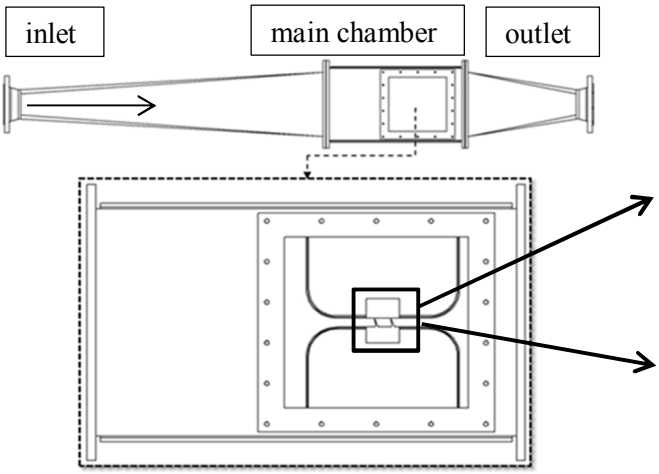

Figure 2. View of the stationary test rig.

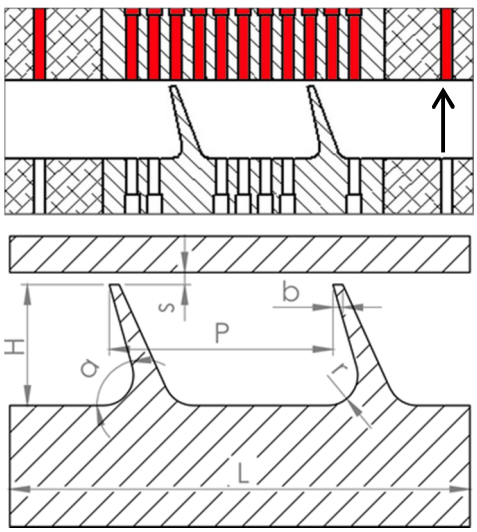

Figure 3. The geometry of examined labyrinth seal.

Table 2. Dimensions of the labyrinth seal

Dimension	Value	Dimension	Value
H/b	12.5	r/b	1.875
P/b	23.19	a	20°
L/b	47.5	s	0.6, 0.75, 1 mm

2.2. Data acquisition system

The measurement system may be divided into several subsystems. The first is the air installation measurement subsystem. It allows the assessment of the blower operation conditions and provides operating information, like bearing temperatures, outlet air temperature and pressure in the vessel and pipeline. The second is the measurement subsystem of the test rig. The quantities measured therein are strictly related to the sealing model operation. The test rig system allows to measure the inlet air velocity, pressure differences, static pressure and temperature distribution along the investigated structure. Accuracy of velocity measurement done by Schmidt 20.500 thermal anemometer does not exceed 2 % measured value, pressure is measured by PC-28 Aplisens pressure transducer with accuracy of ±256 Pa, temperature measurement accuracy, done by means of TTP-TKb, J thermocouple, stands at 0.5°C at 100°C. Investigated clearances has been evaluated using normalised blade feelers. The execution elements and the data acquisition process are managed by a LabView handler co-operating with a PC class computer. The handler was specially developed for the needs of this project. The measuring stand and the software make up an open system that may be developed further by connecting more measuring clusters and modules for a program-based analysis and visualization of data. For results evaluation, about 1000 samples is taken, which corresponds to 90 seconds of measurement.

2.3. Hot Wire Anemometry calibration against Laser Doppler Anemometry

The mass flow was measured using a technique based on the measurement of the stream velocity in a certain point of the flow cross-section. Using the information about the local velocity and knowing of the velocity profile and the flow cross-section size as well as the calibration coefficients determined experimentally, it is possible to find the volume flow of the medium.

Within this project, the stream local velocity was determined using a Schmidt 20.500 thermal anemometer installed in the stand inlet pipe. Pitot tubes were also used for control purposes. The velocity profiles in the pipeline were determined using an LDA anemometer made by Dantec. The LDA technique is characterized by high measuring accuracy and may be treated as a model tool for the stream velocity determination. The velocity profiles, obtained from the measurement (Fig. 4) were used to determine calibration coefficients, which made it possible to calibrate the thermal anemometry probe and find the volume flow rate. The calibration was verified by additional LDA-based determination of velocity profiles before the seal structure for a few selected pressure ratios. The error in the post-calibration volume flow determination does not exceed 2% of the measured value. The manufactures pre calibration correction factor is in range 0.72 – 0.73. Presented procedure made it possible to enhance the measurement accuracy.

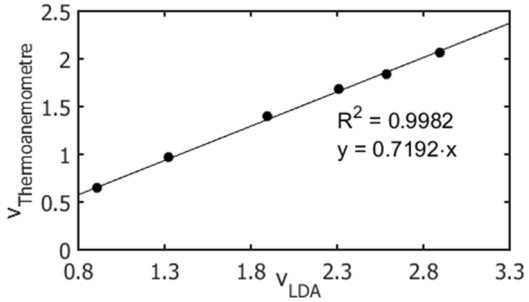

Figure 4. Results of Hot Wire Anemometer measurement against LDA.

3. CFD approach

This section presents the methodology of CFD computations of the flow through the seal model. The aim of the numerical analyses was to determine the air mass flow and the pressure distribution along the seal, especially in the area of the measuring hole location. A simple model of the seal was used for this purpose. Its view is shown in Fig. 5. The clearance between the fin tip and the casing is the same as in experiment, and the width – 5.5 mm, with periodicity boundary condition. These values make it possible to limit the number of the domain elements, ensuring a short computation time and keeping high convergence of residues. Consequently, the velocity components in the circumferential direction are practically eliminated and the model may be considered as a two-dimensional one. The model presented below was used in a further stage to generate the mesh. Computational mesh was generated in ICEM-CFD software, as fully structured. The correct solution to the flow patterns should be mesh-independent. To check this property, a numerical study with seven different mesh sizes with 105k, 167k, 554k, 1.1M, 8.9M, 17.5M and 38.8M grid nodes were used for the mesh dependence tests. The initial mesh with 105k nodes was not refined entirely, but only in regions with greater parameter gradients. The deviation between results for meshes 167k to 38.8M was less than 1% (C_D = 0.591 – 0.605). Although C_D value for initial mesh with 105k nodes was over estimated (C_D = 0.62). This indicates that acceptable tolerance was reached, and the 167k-node mesh can be used for a further analysis. Mesh employed for this analysis is shown in Fig. 6. The mesh has the maximum value of y^+ less than 2, but in the regions close to the rotor walls – $y^+ << 1$.

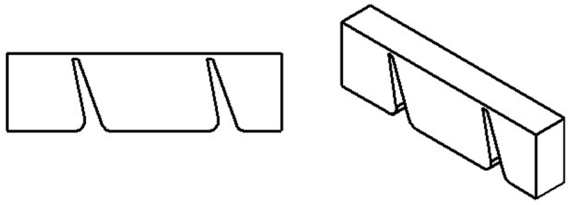

Figure 5. Geometry of CFD model employed for CFD analysis.

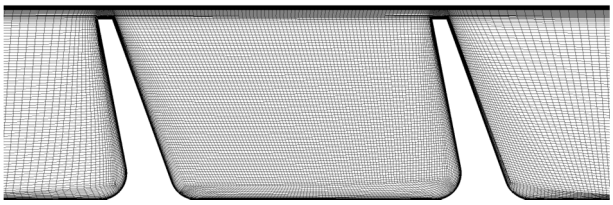

Figure 6. Final mesh of fluid domain above labyrinth structure.

The computations were performed using the commercial code Ansys CFX 16.2 using steady state scheme with Shear Stress Transport turbulence model. Boundary conditions corresponded to the measurements conditions. The working medium was dry air treated as perfect ideal gas. Moreover, the Sutherland formula was applied to determine dynamic viscosity and thermal conductivity as a function of temperature. Due to the fact that, especially after behind the seal second fin, the stream accelerated considerably causing turbulence in the outlet area, the outlet channel was lengthened. Such an approach eliminates the impact of boundary conditions on the flow structure in the sealing and on the possibility of reverse flow formation on the outlet cross-section. A similar procedure was used in the inlet area, where the swirl forming before in front of the seal first fin could distort the process of inflow onto the sealing.

4. Results evaluation

The operation of labyrinth seals is described in literature using dimensionless parameters. One of the most common ones is the discharge coefficient – C_D, which is the ratio of the current mass flow – measured or being the result of numerical calculations – to the mass flow resulting from ideal expansion in a nozzle with a surface area equal to the surface area of the clearance. It takes account of the inlet total pressure and total temperature at the inlet and the pressure ratio forcing the flow:

$$C_D = \frac{\dot{m}}{m_{id}} \tag{2}$$

$$m_{id} = \frac{p_{0,in} \cdot A}{\sqrt{T_{0,in}}} \left(\frac{2\kappa}{R(\kappa - 1)} \left[\left(\frac{1}{\pi} \right)^{\frac{2}{\kappa}} - \left(\frac{1}{\pi} \right)^{\frac{\kappa+1}{\kappa}} \right] \right)^{1/2} \tag{3}$$

Moreover, there is flow function Ψ employed, which is defined as follows:

$$\psi = \frac{\dot{m} \cdot \sqrt{T_{0,in}}}{A \cdot p_{0,in}} \tag{4}$$

For comparison, the curve illustrating the history of the ideal flow function Ψ determined from analytical relationships is also presented:

$$\psi_{ideal} = \left(\frac{2\kappa}{R(\kappa - 1)} \left[\left(\frac{1}{\pi} \right)^{\frac{2}{\kappa}} - \left(\frac{1}{\pi} \right)^{\frac{\kappa+1}{\kappa}} \right] \right)^{1/2} \tag{5}$$

4.1. Flow indicators evaluation

In this subsection, flow indicators – discharge coefficient C_D , flow function Ψ and flow function for ideal parameters Ψ_{ideal} described by equations (2-5) have been presented. Mentioned results show high repeatability of obtained results for mentioned values of clearance. Marked errorbars have been evaluated using the total differential method . It has to be noticed here that each measurement was preceded by disassembling and assembling of the sealing, what was associated with setting of the clearance. Average measurement uncertainty does not exceed 2.5% of C_D or Ψ for clearance s = 1mm, 3.5% for s = 0.75 mm and 4.5% for s = 0.6 mm. Discharge coefficient C_D, as well as Ψ values rise with pressure ratio. For higher clearances, the higher flow indicators were obtained. This is a result of higher mass flow rate in structure with higher clearance, as well as lower losses caused by flow through narrow gap. For comparison, characteristics of discharge coefficient and flow function, for labyrinth seal with smooth land, obtained by means of CFD simulations has also been presented (figures 7, 8). Results from numerical simulations were similar to experimental ones. Average difference between experiment and CFD stood below the uncertainty of measurement.

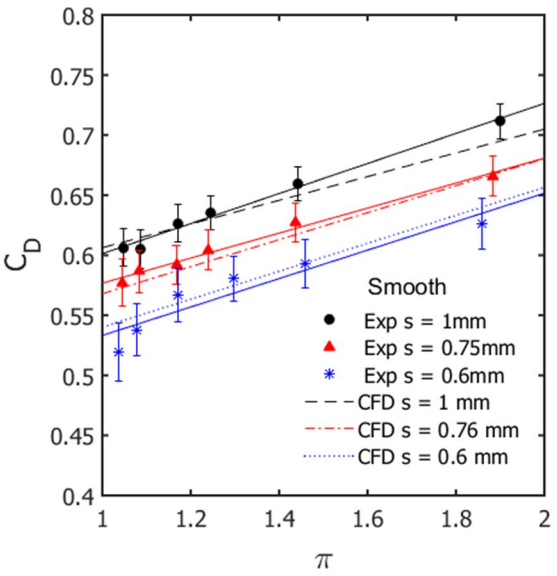

Figure 7. Discharge coefficient with pressure ratio – experiment and CFD.

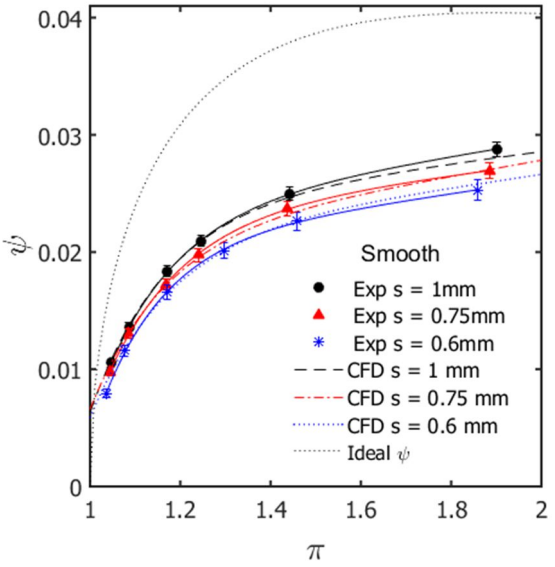

Figure 8. Flow function with pressure ratio – experiment, CFD and ideal value.

4.2. Relative pressure distribution

Figures 9-12 present distributions of static pressure to inlet total pressure ratio along the seal found experimentally for the upper wall. An accurate configuration of the applied sealing is also marked in the figures. Distances marked as x correspond to axial position from the beginning of the labyrinth seal element. Pressure drop measured at first fin is much higher than pressure drop at second fin. This

phenomena is stronger for higher clearance – in case with s = 1 mm, pressure in cavity between fins, is almost the same as behind the second fin. This effect is visible for pressure ratios lower than $\pi = 1.4$. Furthermore, in front of second fin, at distance x = 25 mm some static pressure growth has been measured. This effect is mostly caused by velocity drop. Experimental data have been compared with CFD results. The comparison shows some disagreement between experimental and numerical results. Although the tendencies are similar, the CFD results under predict the static pressure value along the structure. The reason of this differences is still being investigated.

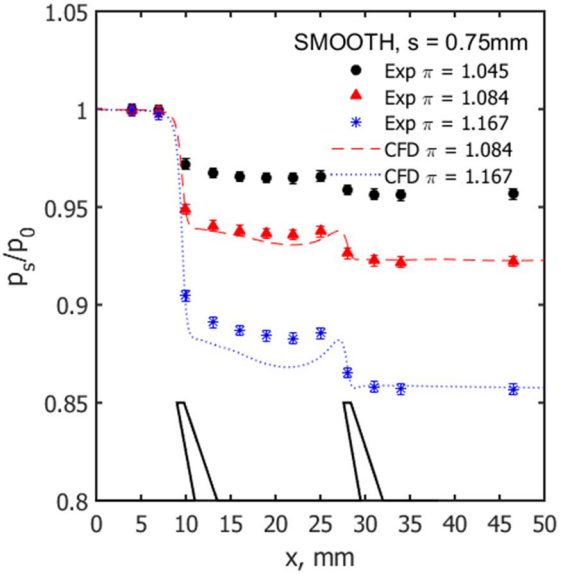

Figure 9. Static pressure distribution for smooth s = 0.75 mm, by low pressure ratios.

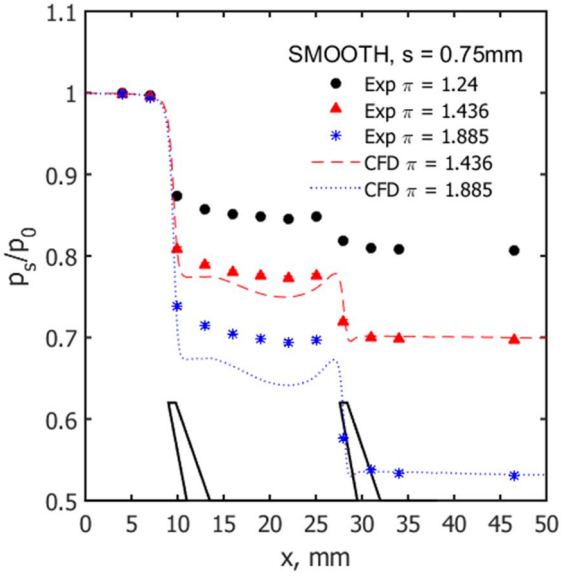

Figure 10. Static pressure distribution for smooth s = 0.75 mm, by high pressure ratios

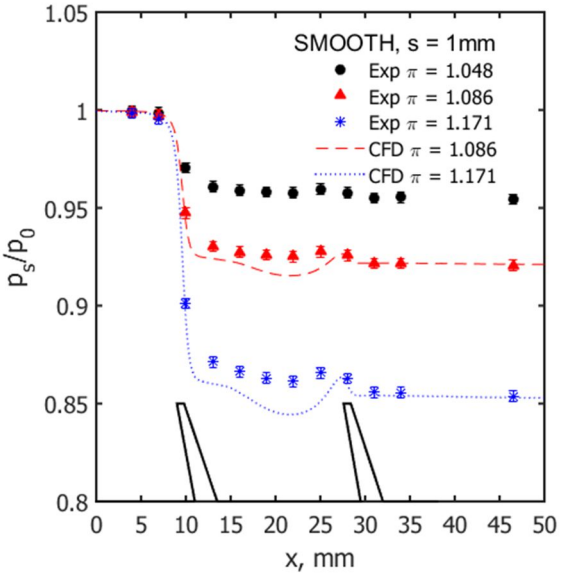

Figure 11. Static pressure distribution for smooth s = 1 mm, by low pressure ratios.

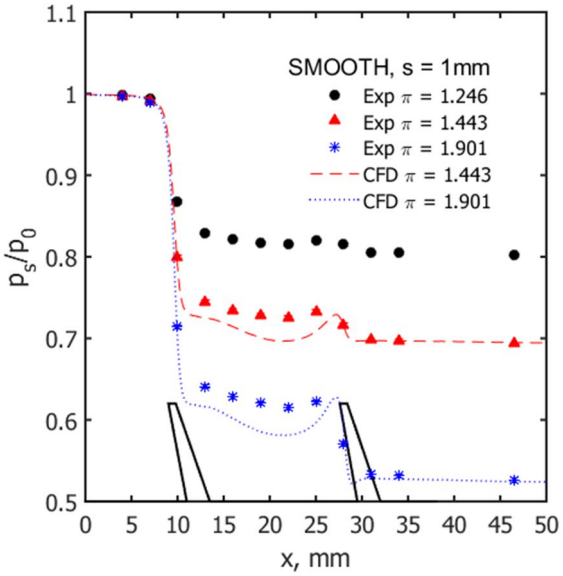

Figure 12. Static pressure distribution for smooth s = 1 mm, by high pressure ratios.

5. Summary and final remarks

In this paper description of experimental test rig for investigation of the flow through the sealing with different architecture has been presented. Together with a design of experimental facility a measurement system and CFD approach have been described. The results of the measurements for one sealing configuration with various clearances have been presented. On the basis of the performed measurements and CFD calculations one can draw the following main conclusions:

- Mass flow measurements by mean of thermo-anemometer have been calibrated against the LDA measurements of the velocity profile, what gives a very high accuracy, which is desirable in case of low mass flow rate measurement.
- Average measurement uncertainty stood below 2 – 4.5%, depending on the clearance size.
- CFD calculations met agreement in case of the flow indicators evaluation, although in case of the static pressure measurement, the CFD code underestimates the pressure values.

Further work will focus on more detailed CFD analysis, for explanation the static pressure behaviour, as well as experimental investigation exploiting different labyrinth seals structures.

Acknowledgments

This work was supported by the National Centre for Research and Development and Avio Polska within the Innolot Programme INNOLOT/I/11/NCBiR/2014, project Coopernik SEK-13/RIE-5/2014.

References

[1] H. L. Stocker, D. M. Cox and G. F. Holle, "Aerodynamic performance of conventional and advanced design labyrinth seals with solid-smooth abradable, and honeycomb lands," NASA-CR-135307, 1977.

[2] Kim T S Kang Y and Moon H K 2008 *Aerodynamic Performance of Double Sided Labyrinth Seals*, 4th International Symposium on Fluid Machinery and Fluid Engineering, p. 377

[3] Massini D Facchini B Micio M Bianchini C Ceccherini A and Innocenti L 2014 *Analysis of flat plate honeycomb seals aerodynamic losses: effects of clearance,* 68th CITMEA, p. 502

[4] V. Schramm, K. Willenborg, S. Kim and S. Wittig, "Influence of a Honeycomb Facing on the Flow Through a Stepped Labyrinth Seal," Journal of Engineering for Gas Turbines and Power, vol. 124, pp. 140-146, January 2002.

[5] J. Li, S. Kong, X. Yan, S. Obi and Z. Feng, "Numerical Investigations on Leakage Performance of the Rotating Labyrinth Honeycomb Seal," Journal of Engineering for Gas Turbines and Power, vol. 132, no. 062501, March 2010.

[6] J. Denecke, V. Schramm, S. Kim and W. S., "Influence of Rub-Grooves on Labyrinth Seal Leakage," Journal of Turbomachinery, vol. 123, pp. 387-393, April 2003.

[7] M.-O. Biester, L. Mueller, J. R. Seume and Y. Guendogdu, "GT2011-45883 Time-Resolved Numerical Investigation of the Interaction of Labyrinth Seal Leakage and Main-Flow in a 1.5-Stage LP Turbine," Proceedings of the ASME Turbo Expo 2013, vol. 5, pp. 1623-1632, June 2011.

[8] J. Denecke, K. Dullenkopf, W. S. and H.-J. Bauer, "GT2005-68677 Experimental Investigation Of The Total Temperature Increase And Swirl Development In Rotating Labyrinth Seals," Proceedings of ASME Turbo Expo 2005 -Power for Land, Sea, and Air, vol. 3, pp. 1161-1171, July 2005.